NATIONAL ADVISORY COMMITTEE FOR AERONAUTICS

TECHNICAL NOTE 3524

THE EFFECT OF REYNOLDS NUMBER ON THE STALLING

CHARACTERISTICS AND PRESSURE DISTRIBUTIONS

OF FOUR MODERATELY THIN AIRFOIL SECTIONS

By George B. McCullough

Ames Aeronautical Laboratory
Moffett Field, Calif.

NACA

Washington

November 1955

AFMDC

NATIONAL ADVISORY COMMITTEE FOR AERONAUTICS

TECHNICAL NOTE 3524

THE EFFECT OF REYNOLDS NUMBER ON THE STALLING

CHARACTERISTICS AND PRESSURE DISTRIBUTIONS

OF FOUR MODERATELY THIN AIRFOIL SECTIONS

By George B. McCullough

SUMMARY

Low-speed measurements of the lift, drag, pitching moment, and pressure distribution of the NACA 0008, 0007.5, 0007, and 0006 airfoil sections are presented for Reynolds numbers from 1.5 to 6 million. It is shown that the flow over these airfoil sections changed from the type which precedes leading-edge stall to the type which precedes thin-airfoil stall at some lift coefficient which depended on the Reynolds number and on the airfoil thickness ratio. An increase of either of these two variables increased the lift corresponding to the flow change until, for the thicker sections at least, maximum lift was attained before the flow change occurred. It is possible, therefore, for airfoil sections in a certain range of thickness ratios to stall with either the thin-airfoil or leading-edge type of stall, depending on the Reynolds number. For the NACA 4-digit family of airfoils there were no abrupt variations of maximum lift accompanying the change of stall.

INTRODUCTION

A previous report (ref. 1) describes the low-speed stalling characteristics of airfoil sections with thickness ratios from 4.23 to 18 percent of the chord. The stalling characteristics were divided into three types based on wind-tunnel studies made at a Reynolds number of 5.8 million. The three types were called: trailing-edge stall, leading-edge stall, and thin-airfoil stall. The latter two are of particular interest because they are inherent to the thinner airfoils of current usage, whereas trailing-edge stall is inherent to the thicker conventional airfoils, and is therefore more familiar.

Leading-edge stall was described as an abrupt flow separation near the leading edge generally without subsequent reattachment. For angles of attack up to and including that for maximum lift the pressure distribution over the airfoil was essentially that for unseparated potential flow except for relatively minor effects due to the boundary layer and a small region of separated flow near the leading edge commonly referred to as

the laminar-separation bubble. Thin-airfoil stall, on the other hand, was described as being preceded by flow separation at the leading edge with reattachment at a point which moved progressively rearward with increasing angle of attack. The two types of stall are similar in that both originate with flow separation from the leading edge, but are radically different in the type of flow which precedes the stall. The conditions which determined the type of flow were not apparent, and hence were the subject of considerable speculation. It was planned, therefore, to undertake detailed measurements of the two flows in an attempt to arrive at a better understanding of their differences.

In this connection, it had been observed that certain thin, round-nose airfoils experienced a change in flow at some critical angle of attack prior to the attainment of maximum lift. For angles of attack less than the critical the flow was unseparated. From the critical angle of attack to the angle of attack for maximum lift the flow separated from the leading edge and reattached at a point which moved aft with increasing angle of attack.

It had also been observed that increasing the Reynolds number increased the angle of attack at which the flow change occurred; hence it seemed logical that for a sufficiently large Reynolds number the flow change would be delayed until the section stalled with the abrupt or leading-edge type of stall. Such a change in stalling characteristics was actually observed for the NACA 64A010 airfoil section (data unpublished), but the Reynolds number, and consequently the dynamic pressure, corresponding to thin-airfoil stall was so low as to preclude satisfactory measurements. A small increase of Reynolds number produced the change to leading-edge stall which was accompanied by a marked increase of maximum lift.

The possibility of obtaining both the thin-airfoil and leading-edge types of stall on the same airfoil model at different Reynolds numbers offered an attractive scheme for studying the two flows because it would eliminate the effects of differences in airfoil geometry, and permit measurements in both flow regimes with the same experimental setup. For this purpose a model of the NACA 0008 section was so constructed that its thickness could be reduced. Measurements were made in one of the Ames 7- by 10-foot wind tunnels of the lift, drag, pitching moment, and pressure distribution for various values of Reynolds number from 1.5 to 6 million. Then the model was successively recontoured to the NACA 0007.5 and 0007 profiles and the measurements were repeated. To extend the range of thickness ratios, a similar investigation was made with an existing NACA 0006 airfoil.

NOTATION

The symbols used in this report are defined as follows:

c   wing chord, ft

c_d section profile-drag coefficient, $\dfrac{D}{qc}$, including drag of circular end plates

c_l section lift coefficient, $\dfrac{L}{qc}$

c_m section pitching-moment coefficient, $\dfrac{M}{qc^2}$

c_N section normal-force coefficient, $\dfrac{N}{qc}$

D   drag per unit span, lb

L   lift per unit span, lb

M   pitching moment about the 0.25c axis per unit span, lb-ft

N   normal force per unit span, lb

p   local static pressure, lb/sq ft

p_0 free-stream static pressure, lb/sq ft

P   pressure coefficient, $\dfrac{p-p_0}{q}$

q   free-stream dynamic pressure, lb/sq ft

R   Reynolds number based on wing chord

u   local velocity within the boundary layer, ft/sec

U   local velocity outside boundary layer, ft/sec

x   distance from airfoil leading edge parallel to chord line, ft

y   distance above airfoil normal to surface, ft

α angle of attack, deg

MODELS AND TESTS

Models

The basic model was constructed of wood with numerous midspan pres-
sure orifices so installed that the thickness of the model could be
reduced from 8 to 7 percent without damage to the orifices. The chord
was 5 feet and the span 7 feet. Attached to the ends of the model were
circular plates which formed part of the tunnel floor and ceiling.

The NACA 0006 airfoil was of 4-1/2-foot chord and was not as accu-
rately contoured as the 5-foot-chord model nor did it contain as many
orifices near the leading edge.

Tests

Most of the force and moment measurements were made for specific
values of Reynolds number with angle of attack as the variable. The
corresponding pressure-distribution measurements usually were made inde-
pendently and for fewer values of Reynolds number. Some data were
obtained, however, for various constant angles of attack with Reynolds
number as the variable. For these tests the pressure-distribution
measurements were made simultaneously with the force measurements. For
the 5-foot-chord model the Reynolds number range was from 1.5 million to
6 million. The corresponding Mach number range was from 0.03 to 0.17.
For the 4-1/2-foot-chord model the Reynolds number range was from 1.9
million to 6.8 million, and the corresponding Mach number range was from
0.05 to 0.22.

The force and moment data were measured by means of the wind-tunnel
balance system, and hence include the unknown tares of the end plates.
Previous experience has shown that the lift and moment tares are negligibly
small. The drag tares, however, are large and vary with angle of attack.
The data have not been corrected for tunnel-wall constraint or the effects
of compressibility,[1] and in this respect are comparable to the data of
reference 1.

Measurements were made of the boundary-layer velocity profiles on
the NACA 0007 airfoil by means of the usual small rakes of total- and
static-pressure tubes.

---

[1]The corrections usually applied to the data are those described
in reference 2. The effect of the corrections is to increase the angle
of attack and to reduce the values of the lift,drag, and moment coef-
ficients. The effect of the Mach number variation would be to reduce
the variation of lift-curve slope with Reynolds number shown by the
uncorrected data.

RESULTS AND DISCUSSION

Force and Moment Characteristics

The lift, drag, and pitching-moment data for the four airfoil sections are presented in figure 1. In the lift curves for the NACA 0006 section (fig. 1(d)) small jogs or discontinuities can be noted prior to the attainment of maximum lift. Corresponding to each of these discontinuities is a sudden increase of drag and a positive shift of the pitching moment followed by a strong negative trend. A similar behavior was observed for the NACA 64A006 section (ref. 3), and is discussed in reference 1. It was shown that the discontinuity was the result of the appearance of an extensive region of separated flow near the leading edge. The same sort of flow change occurred on the airfoils of the present investigation although not as far below maximum lift as was the case for the NACA 64A006 section.

For the NACA 0006 section, the flow change occurred immediately above 6° angle of attack for all Reynolds numbers. The effect of increasing Reynolds number was to increase slightly the lift coefficient at which the flow changed, but the change was always well below maximum lift, and the stall was of the thin-airfoil type for all Reynolds numbers.

For the thicker airfoil sections the effect of increasing Reynolds number was to increase not only the lift coefficient but also the angle of attack at which the flow change occurred so that there was a Reynolds number for which the change coincided with maximum lift. With further increases of Reynolds number the airfoil stalled with the leading-edge type of stall. For the NACA 0007 section this point was nearly reached at a Reynolds number of 6 million, and for the 0007.5 and 0008 sections the type of stall changed at a Reynolds number of about 3 million.

It should be mentioned that the results, insofar as the angle of attack for the flow change is concerned, were not always repeatable. Reruns of force measurements or separate runs for the purpose of pressure-distribution measurements sometimes gave results which differed by 1° in the angle of attack for the flow change. One such inconsistency can be seen in the data for the NACA 0008 airfoil at a Reynolds number of 1.5 million (fig. 1(a)). By comparison with the lift curves for the higher Reynolds numbers it would be expected that the flow change would occur at a lower value of lift coefficient than that shown by the unflagged symbols. Only one constant-Reynolds-number run was made, but a few runs were made with decreasing Reynolds number and constant angles of attack. The flagged symbols represent values obtained by cross-plotting the constant angle-of-attack data, and show a discontinuity at about the expected value of lift coefficient. Cross-plotted data are also shown by the flagged symbols for a Reynolds number of 2 million. For the higher Reynolds numbers the cross-plotted data agreed well with the variable angle-of-attack data and are not shown.

A summary of the effect of Reynolds number on maximum lift and on the lift coefficient corresponding to the flow change is shown in figure 2. There is a tendency for the lift coefficient corresponding to the flow change to approach maximum lift more slowly with increasing Reynolds number for the thinner sections than for the thicker sections.

Pressure Distribution

Pressure-distribution data for the four airfoil sections at Reynolds numbers of 2 million, 4 million, and 6 million are given in tables I to IV. For each airfoil, data are given for the highest angle of attack common to all Reynolds numbers for which completely attached flow was measured, and for enough additional angles of attack to bracket the flow change in each case. Also listed in the table are values of the normal-force coefficient obtained by integrating the pressure diagrams.

The effect of the change in flow on the chordwise distribution of pressure is illustrated in figure 3. The two pressure distributions are for the NACA 0007.5 airfoil at angles of attack of 9° and 10° and a Reynolds number of 3 million. The pressure distribution for 9° angle of attack corresponds to the completely attached flow prior to the flow change, and the pressure distribution for 10° angle of attack corresponds to partially separated flow. Both diagrams represent almost exactly the same value of lift.

The abruptness of the flow change is shown in figure 4 in which the pressures at several chordwise stations are plotted as a function of angle of attack. It happened that both types of flow were obtained at an angle of attack of 9°, whereas 8° was the highest angle of attack for which unseparated flow was obtained in the force measurements. The effect of the small bubble of laminar separation (discussed in ref. 1) can be seen in the variations of pressure with angle of attack for the 0.5-, 1.0-, and 1.5-percent-chord stations. When the flow change occurred the pressures near the leading edge increased abruptly and continued to increase with increasing angle of attack but at a slower rate. Because of the region of separated flow, the pressures over the forward portion of the airfoil were of nearly the same value. The pressures over the rear portion of the airfoil were less severely affected by the flow change, and decreased with increasing angle of attack beyond the flow change. This redistribution of the chordwise loading accounts for the increasing negative trend of the pitching moment. A similar redistribution of loading for the NACA 64A006 airfoil is described in reference 3.

Hysteresis Effect

One test was made to ascertain the effect of decreasing and then increasing the Reynolds number at a constant angle of attack. This was made with the NACA 0007 airfoil at an angle of attack of 7.5° which was below the angle of attack for the flow change for Reynolds numbers greater than 2 million (fig. 1(c)). The test was started with completely unseparated flow over the model and a Reynolds number of 6 million. The Reynolds number was progressively reduced to 1.5 million, and then progressively increased to 6 million without changing angle of attack or stopping the tunnel. The results of lift measurements are shown in figure 5(a).

The lift coefficient decreased slightly with decreasing Reynolds number to 2.2 million, then dropped abruptly at a Reynolds number of 2.0 million and remained at about the same value at a Reynolds number of 1.5 million. The values of lift coefficient agree well with values from the tests at constant Reynolds numbers except for the point at a Reynolds number of 2.0 million. This difference is due to the fact that the flow remained attached for the variable angle-of-attack test but was partially separated for the variable Reynolds number test.

With increasing Reynolds number the lift coefficient increased slowly, but failed to achieve the abrupt increase which would be expected to accompany the re-establishment of unseparated flow. At a Reynolds number of 6 million the terminal value of lift coefficient was about 0.05 below the initial value.

The variations of pressure coefficient with Reynolds number for several stations on the upper surface of the airfoil are shown in figure 5(b). The abrupt increase of pressure near the leading edge when the Reynolds number was reduced from 2.2 million to 2.0 million and the failure of the pressure to attain its original low value when the Reynolds number was increased is clearly evident. The pressure coefficients at 4-percent chord and over the rear 80 percent of the airfoil were relatively unaffected by changes of Reynolds number.

In figure 6 are shown the initial and the final pressure distributions over the first 5-percent chord for a Reynolds number of 6 million. Both show evidence of the small bubble of laminar separation as indicated by the abrupt increase of pressure gradient at about 0.5-percent chord, but are otherwise representative of attached flow. One reason for the failure of the airfoil to regain its original pressure distribution could be the flow conditions in the wind tunnel. Experience has shown that flow separation is frequently more extensive at the ends of two-dimensional models than near midspan because of so-called end effects probably due to the boundary layer on the tunnel walls. Once flow separation was established across the span of the model by decreasing the Reynolds number, it is possible that separation near the ends of the model was not eliminated when the Reynolds number was increased to 6 million. The resultant

spanwise variation of pressure could cause the pressures measured at the
midspan pressure orifices to be higher than was the case with more nearly
two-dimensional flow.

Boundary-Layer Characteristics

Some representative boundary-layer measurements made on the NACA 0007
airfoil for a Reynolds number of 2 million are shown in figure 7. Profiles
are shown for three stations for 7° and 8° angle of attack which correspond
to conditions before and after the flow change. The station at 2.5-percent
chord was in the region of separated flow for an angle of attack of 8°,
and hence the shape of the lower portion of the profile is uncertain
because the total-pressure tubes of the rake were in a region of unsteady
flow and were incapable of reading the true local total pressure. The
profiles at the 50- and 90-percent chord were in a region of attached flow
and show the pronounced thickening of the turbulent boundary layer caused
by the separated flow over the forward portion of the airfoil.

In the Appendix of reference 4 it is shown from detailed pressure-
distribution and boundary-layer measurements on an airfoil section for a
wide range of test conditions that a shoulder or abrupt discontinuity of
curvature in the pressure distribution corresponds to the first appearance
of completely turbulent flow in the detached boundary layer enveloping the
small bubble of laminar separation. Similar discontinuities can be seen
in the pressure distributions shown in figure 8 for the NACA 0007.5 airfoil
at an angle of attack of 7° and several Reynolds numbers The lack of a
large number of pressure orifices in the region of transition necessitated
considerable arbitrariness in fairing the curves, but the forward progres-
sion of the transition region with increasing Reynolds number is plainly
evident. Cross plots of the data in figure 8 and of similar data for other
angles of attack are shown in figure 9. The forward movement of the region
of transition, and hence the small bubble of laminar separation, with
increasing angle of attack was relatively rapid at first, but the rate of
progression decreased at the higher angles. Since the indicated positions
of transition are well forward on the nose radius of the airfoil, their
actual movement around the curved surface was greater than is indicated
by the figure.

Also shown in the figure is the approximate boundary for the change
of flow. When this boundary was reached, either by increasing the angle
of attack or by reducing Reynolds number, the flow changed from essentially
unseparated flow to the type which precedes thin-airfoil stall or to
leading-edge stall, depending on the Reynolds number.

CONCLUDING REMARKS

Tests of four symmetrical airfoil sections in the thickness range from 6 to 8 percent of the chord have indicated that the nature of their stalls depends on the Reynolds number. In general, low Reynolds numbers are favorable to the thin-airfoil type of stall, and high Reynolds numbers are favorable to the leading-edge type of stall. For the NACA 4-digit series of airfoil sections, the effect of a change in the stall on maximum lift was small, but the Reynolds number at which the change occurred was sensitive to small changes of thickness ratio. For this reason it was deemed impractical to attempt detailed measurements of the two types of separated flow using a single airfoil section in the critical range of thickness ratios.

Ames Aeronautical Laboratory
     National Advisory Committee for Aeronautics
          Moffett Field, Calif., Aug. 29, 1955.

REFERENCES

1. McCullough, George B., and Gault, Donald E.: Examples of Three Representative Types of Airfoil-Section Stall at Low Speed. NACA TN 2502, 1951.

2. Allen, H. Julian, and Vincenti, Walter G.: Wall Interference in a Two-Dimensional-Flow Wind Tunnel, With Consideration of the Effect of Compressibility. NACA Rep. 782, 1944.

3. McCullough, George B , and Gault, Donald E.: Boundary-Layer and Stalling Characteristics of the NACA 64A006 Airfoil Section. NACA TN 1923, 1949.

4. Gault, Donald E.: An Experimental Investigation of Regions of Separated Laminar Flow. NACA TN 3505, 1955.

TABLE I.- NACA 0008 AIRFOIL

Chordwise station, percent chord	Pressure coefficient, P															
	R = 2,000,000				R = 4,000,000						R = 6,000,000					
	$\alpha=8.0°$; $c_N=0.918$		$\alpha=8.5°$; $c_N=0.936$		$\alpha=8.0°$; $c_N=0.924$		$\alpha=9.0°$; $c_N=1.050$		$\alpha=10.0°$; $c_N=0.956$		$\alpha=8.0°$; $c_N=0.942$		$\alpha=9.0°$; $c_N=1.028$		$\alpha=10.0°$; $c_N=0.976$	
	Upper	Lower	Upper	Lower	Upper	Lower	Upper	Lower	Upper	Lower	Upper	Lower	Upper	Lower	Upper	Lower
0	-5.55	- - -	-2.90	- - -	-6.07	- - -	-7.93	- - -	-2.10	- - -	-6.38	- - -	-7.88	- - -	-2.54	- - -
.03	-6.90	-2.35	-3.26	-1.00	-7.54	-2.64	-9.56	-3.81	-2.24	-.68	-7.91	-2.72	-9.58	-3.70	-2.49	-.83
.1	-7.00	-1.35	-3.05	-.37	-7.66	-1.54	-9.49	-2.46	-2.00	-.17	-8.02	-1.60	-9.42	-2.37	-2.17	-.28
.2	-6.45	-.35	-2.95	.21	-7.17	-.51	-8.85	-1.17	-1.98	.32	-7.53	-.57	-8.90	-1.11	-2.23	.24
.33	-6.05	.15	-2.95	.58	-6.77	.07	-8.46	-.42	-1.93	.56	-7.08	.03	-8.23	-.37	-2.04	.54
.5	-5.90	.60	-2.90	.84	-5.61	.46	-6.51	.12	-1.88	.78	-5.66	.44	-6.46	.14	-1.93	.72
.67	-5.65	.85	-2.84	.93	-4.90	.72	-5.88	.49	-1.85	.88	-5.11	.70	-5.87	.50	-1.87	.68
.83	-4.30	.95	-2.74	1.00	-4.66	.85	-5.56	.68	-1.83	.93	-4.86	.84	-5.53	.70	-1.85	.94
1.00	-4.05	1.00	-2.68	1.05	-4.49	.93	-5.32	.83	-1.81	.95	-4.63	.93	-5.27	.83	-1.81	.97
1.5	-3.65	1.05	-2.63	1.05	-3.94	1.00	-4.61	.98	-1.78	.98	-4.05	1.00	-4.56	.98	-1.74	.99
2	-3.25	1.05	-2.53	1.00	-3.43	1.00	-3.98	1.00	-1.74	.95	-3.55	1.00	-3.93	1.00	-1.70	.96
2.5	-2.90	1.00	-2.58	.95	-3.07	.97	-3.56	1.00	-1.73	.90	-3.15	.98	-3.51	1.00	-1.76	.93
3	-2.60	.95	-2.42	.90	-2.77	.94	-3.20	.98	-1.71	.85	-2.85	.94	-3.16	.98	-1.67	.88
4	-2.30	.85	-2.37	.84	-2.42	.85	-2.78	.93	-1.72	.78	-2.47	.87	-2.76	.93	-1.65	.81
5	-2.20	.80	-2.32	.74	-2.20	.78	-2.50	.85	-1.72	.71	-2.24	.80	-2.47	.88	-1.65	.74
7.5	-1.65	.65	-2.11	.63	-1.76	.63	-2.00	.73	-1.71	.59	-1.79	.66	-1.96	.73	-1.61	.62
10	-1.45	.55	-1.89	.53	-1.51	.56	-1.71	.63	-1.66	.51	-1.55	.56	-1.68	.63	-1.56	.53
12.5	-1.25	- - -	-1.68	- - -	-1.34	- - -	-1.51	- - -	-1.61	- - -	-1.37	- - -	-1.49	- - -	-1.50	- - -
15	-1.15	.45	-1.47	.42	-1.21	.43	-1.37	.49	-1.54	.39	-1.23	.44	-1.34	.50	-1.43	.40
20	-.95	.35	-1.16	.32	-1.01	.34	-1.15	.39	-1.37	.29	-1.04	.36	-1.12	.41	-1.30	.32
25	-.85	.30	-.95	.26	-.88	.29	-.99	.34	-1.22	.23	-.90	.30	-.96	.35	-1.17	.26
30	-.75	.25	-.79	.21	-.78	.24	-.85	.29	-1.07	.20	-.79	.26	-.84	.30	-1.05	.22
35	-.65	.25	-.68	.16	-.68	.21	-.75	.27	-.95	.15	-.69	.23	-.74	.27	-.94	.19
40	-.55	.25	-.63	.16	-.61	.20	-.66	.22	-.83	.13	-.62	.20	-.65	.24	-.85	.16
45	-.50	.20	-.53	.11	-.54	.16	-.59	.20	-.73	.10	-.55	.18	-.57	.22	-.73	.14
50	-.45	.15	-.47	.11	-.48	.15	-.51	.18	-.66	.09	-.47	.17	-.50	.20	-.68	.11
55	-.35	.15	-.42	.11	-.42	.15	-.45	.17	-.59	.07	-.41	.15	-.43	.18	-.61	.09
60	-.30	.15	-.37	.11	-.37	.12	-.39	.15	-.51	.05	-.37	.14	-.38	.17	-.54	.07
65	-.25	.15	-.32	.11	-.31	.12	-.33	.15	-.46	.02	-.31	.13	-.32	.16	-.49	.06
70	-.20	.15	-.26	.11	-.24	.12	-.27	.15	-.42	.02	-.25	.12	-.26	.15	-.42	.05
75	-.15	.15	-.21	.11	-.20	.11	-.21	.12	-.34	0	-.20	.12	-.21	.14	-.38	.03
80	-.10	.15	-.16	.11	-.15	.11	-.17	.12	-.32	-.01	-.14	.12	-.14	.14	-.34	.01
85	-.05	.15	-.11	.05	-.10	.10	-.10	.11	-.29	-.05	-.09	.10	-.09	.11	-.30	-.03
90	0	.15	-.11	.05	-.04	.09	-.05	.10	-.24	-.07	-.03	.09	-.03	.09	-.25	-.06
95	.05	.15	-.05	0	.02	.10	.02	.10	-.21	-.10	.04	.09	-.04	.10	-.21	-.09

TABLE II.- NACA 0007.5 AIRFOIL

Chordwise station, percent chord	Pressure coefficient, P															
	R = 2,000,000				R = 4,000,000						R = 6,000,000					
	α=8.0°; cN=0.785		α=8.1°; cN=0.757		α=8.0°; cN=0.886		α=9.0°; cN=0.942		α=9.0°; cN=0.886		α=8.0°; cN=0.906		α=9.5°; cN=1.081		α=9.75°; cN=0.953	
	Upper	Lower	Upper	Lower	Upper	Lower	Upper	Lower	Upper	Lower	Upper	Lower	Upper	Lower	Upper	Lower
0	-6.78	---	-2.67	---	-7.65	---	-9.16	---	-2.24	---	-7.90	---	-11.20	---	-2.55	---
.03	-7.50	-1.39	-2.56	-.11	-8.46	-1.68	-9.86	-2.45	-2.03	-.05	-8.82	-1.71	-12.12	-3.14	-2.32	-.28
.1	-6.67	-.33	-2.44	.44	-7.68	-.54	-8.97	-1.08	-2.00	.45	-7.85	-.56	-10.79	-1.56	-2.18	.28
.2	-6.22	.28	-2.44	.67	-7.05	.11	-8.00	-.29	-1.97	.71	-7.20	.73	-9.38	-.64	-2.13	.59
.33	-6.06	.61	-2.44	.67	-6.51	.51	-7.05	.24	-1.97	.87	-6.43	.48	-8.10	-.01	-2.02	.81
.5	-5.78	.78	-2.39	.83	-5.35	-.76	-5.97	.55	-1.92	.95	-5.52	.72	-7.03	.38	-1.93	.91
.67	-4.56	.94	-2.39	.89	-5.05	-.89	-5.66	.74	-1.90	.97	-5.22	.85	-6.61	.61	-1.91	.95
.83	-4.11	.94	-2.39	1.00	-4.84	-.95	-5.37	.87	-1.90	.97	-4.93	.92	-6.21	.76	-1.87	.97
1	-3.94	1.00	-2.33	1.00	-4.50	1.00	-4.95	.97	-1.88	.97	-4.57	.98	-5.72	.94	-1.85	.97
1.5	-3.22	.94	-2.33	.94	-3.60	.97	-3.95	1.00	-1.86	.92	-3.64	.97	-4.56	1.00	-1.79	.93
2	-2.89	.94	-2.33	.89	-3.19	.95	-3.50	.97	-1.86	.87	-3.24	.94	-4.00	1.00	-1.75	.90
2.5	-2.67	.89	-2.28	.89	-2.96	.89	-3.21	.95	-1.86	.82	-3.00	.91	-3.67	.98	-1.74	.85
3	-2.39	.83	-2.22	.78	-2.70	.84	-2.92	.90	-1.84	.74	-2.74	.84	-3.34	.90	-1.72	.78
4	-2.11	.72	-2.22	.72	-2.34	.76	-2.51	.82	-1.83	.68	-2.36	.78	-2.85	.85	-1.70	.71
5	-1.83	.61	-2.17	.56	-2.08	.62	-2.24	.68	-1.83	.57	-2.11	.64	-2.54	.75	-1.70	.59
7.5	-1.50	.56	-1.89	.44	-1.70	.53	-1.82	.61	-1.76	.47	-1.71	.55	-2.03	.65	-1.67	.49
10	-1.28	---	-1.67	---	-1.49	---	-1.58	---	-1.65	---	-1.49	---	-1.75	---	-1.62	---
12.5	-1.11	---	-1.39	---	-1.30	---	-1.40	---	-1.50	---	-1.32	---	-1.54	---	-1.57	---
15	-1.00	.44	-1.17	.39	-1.16	.41	-1.24	.47	-1.47	.37	-1.18	.42	-1.37	.52	-1.51	.37
20	-.83	.33	-.89	.33	-1.00	.38	-1.05	.40	-1.26	.29	-1.00	.34	-1.15	.44	-1.37	.30
25	-.67	.28	-.78	.22	-.87	.26	-.90	.32	-1.08	.24	-.87	.28	-1.00	.37	-1.22	.23
30	-.61	.28	-.61	.22	-.76	.22	-.79	.29	-.92	.18	-.76	.25	-.86	.32	-1.08	.20
35	-.50	.22	-.50	.22	-.66	.18	-.67	.25	-.76	.16	-.66	.21	-.75	.29	-.95	.16
40	-.44	.22	-.44	.22	-.60	.16	-.61	.21	-.66	.13	-.60	.19	-.67	.25	-.84	.13
45	-.39	.17	-.39	.17	-.51	.14	-.53	.18	-.58	.11	-.53	.17	-.59	.23	-.74	.10
50	-.33	.11	-.33	.11	-.46	.11	-.46	.17	-.50	.09	-.47	.15	-.52	.20	-.66	.08
55	-.28	.11	-.22	.11	-.35	.11	-.34	.16	-.37	.08	-.35	.14	---	.19	-.51	.07
60	-.22	.11	-.22	.11	-.35	.11	-.34	.15	-.37	.08	-.35	.12	-.38	.17	-.52	.05
65	-.22	.11	-.22	.11	-.30	.08	-.30	.13	-.32	.05	-.30	.11	-.33	.16	-.45	.03
70	-.17	.11	-.17	.11	-.24	.08	-.24	.13	-.28	.05	-.25	.11	-.27	.15	-.40	.01
75	-.11	---	-.11	---	-.20	---	-.18	---	-.24	---	-.20	---	-.23	---	-.37	---
80	-.11	.11	-.11	.11	-.16	.08	-.15	.11	-.20	.03	-.16	.09	-.17	.11	-.32	-.02
85	-.06	.06	-.06	.11	-.11	.05	-.11	.09	-.16	.01	-.10	.08	-.11	.10	-.28	-.05
90	0	.11	0	.11	-.05	.05	-.04	.09	-.13	0	-.05	.08	-.05	.10	-.24	-.07
95	.06	.06	.06	.06	0	.05	.03	.08	-.12	-.05	.02	.07	.02	.07	-.20	-.10

TABLE III.- NACA 0007 AIRFOIL

Chordwise station, percent chord	Pressure coefficient, P															
	R = 2,000,000				R = 4,000,000						R = 6,000,000					
	α=7.5°; c_N=0.862		α=7.75°; c_N=0.799		α=7.5°; c_N=0.878		α=8.0°; c_N=0.928		α=8.25°; c_N=0.864		α=7.5°; c_N=0.904		α=8.0°; c_N=0.966		α=8.25°; c_N=0.910	
	Upper	Lower	Upper	Lower	Upper	Lower	Upper	Lower	Upper	Lower	Upper	Lower	Upper	Lower	Upper	Lower
0	-6.94	---	-2.47	---	-7.10	---	-8.07	---	-2.39	---	-7.27	---	-8.20	---	-2.96	---
.05	-7.53	---	-2.35	---	-7.75	---	-8.66	---	-2.16	---	-7.91	---	-8.76	---	-2.08	---
.08	---	-3.00	---	-.60	---	-3.15	---	-3.73	---	-.03	---	-3.14	---	-3.79	---	-.96
.15	-7.18	-1.18	-2.12	.10	-7.46	-1.29	-8.24	-1.76	-2.07	---	-7.36	-1.35	-8.22	-1.80	-1.94	-.09
.25	-6.77	---	-2.12	---	-6.77	---	-7.41	---	-2.06	---	-6.91	---	-7.63	---	-1.88	---
.28	---	0	---	.50	---	.12	---	-.38	---	.06	---	.15	---	-.43	---	.49
.38	-6.47	---	-2.12	---	-6.34	---	-7.00	---	-2.03	---	-6.44	---	-6.94	---	-1.82	---
.43	---	.59	---	.70	---	.46	---	.27	---	.61	---	.43	---	.27	---	.74
.58	---	.82	---	.75	---	.71	---	.61	---	.84	---	.70	---	.53	---	.90
.60	-5.88	---	-2.12	---	-5.39	---	-5.67	---	-2.03	---	-5.36	---	-5.71	---	-1.80	---
.77	-4.94	---	-2.12	---	-4.83	---	-4.93	---	-2.02	---	-4.97	---	-5.41	---	-1.66	---
.78	---	.94	---	.80	---	.85	---	.79	---	.93	---	.85	---	.78	---	.96
.90	-4.47	---	-2.12	---	-4.51	---	-4.87	---	-2.00	---	-4.66	---	-5.06	---	-1.66	---
.93	---	.94	---	.80	---	.94	---	.90	---	.99	---	.93	---	.88	---	1.00
1.07	-4.12	---	-2.12	---	-4.16	---	-4.47	---	-1.97	---	-4.27	---	-4.63	---	-1.77	---
1.10	---	.94	---	.80	---	.99	---	.93	---	.99	---	.96	---	.94	---	.99
1.58	-3.47	---	-2.12	---	-3.49	---	-3.76	---	-1.97	---	-3.59	---	-3.86	---	-1.78	---
1.60	---	1.00	---	.80	---	1.00	---	.99	---	.96	---	.99	---	.99	---	.98
2.08	-3.06	---	-2.12	---	-3.09	---	-3.28	---	-1.97	---	-3.16	---	-3.38	---	-1.79	---
2.10	---	.94	---	.80	---	.97	---	.99	---	.91	---	.97	---	.98	---	.94
2.55	-2.77	---	-2.12	---	-2.80	---	-2.98	---	-1.97	---	-2.87	---	-3.07	---	-1.79	---
2.60	---	.88	---	.70	---	.93	---	.96	---	.87	---	.94	---	.96	---	.89
3.08	-2.47	---	-2.06	---	-2.51	---	-2.66	---	-1.97	---	-2.56	---	-2.74	---	-1.79	---
3.12	---	.82	---	.70	---	.88	---	.91	---	.61	---	.90	---	.92	---	.84
4.05	-2.18	---	-2.06	---	-2.17	---	-2.30	---	-1.97	---	-2.22	---	-2.36	---	-1.81	---
4.10	---	.77	---	.60	---	.80	---	.84	---	.72	---	.82	---	.84	---	.77
5.05	-1.94	---	-2.00	---	-1.97	---	-2.07	---	-1.97	---	-2.01	---	-2.13	---	-1.83	---
5.07	---	.71	---	.55	---	.74	---	.77	---	.67	---	.75	---	.78	---	.70
7.57	-1.59	.59	-2.00	.45	-1.61	.59	-1.69	.64	-1.88	.55	-1.64	.62	-1.73	.65	-1.81	.58
10.05	---	.47	---	.40	---	.51	---	.56	---	.46	---	.53	---	.56	---	.49
10.06	-1.35	---	-1.68	---	-1.38	---	-1.44	---	-1.77	---	-1.40	---	-1.48	---	-1.76	---
12.5	-1.18	---	-1.65	---	-1.23	---	-1.27	---	-1.62	---	-1.25	---	-1.32	---	-1.68	---
15	-1.06	.35	-1.47	.30	-1.12	.38	-1.16	.41	-1.51	.35	-1.14	.41	-1.19	.43	-1.58	.38
20	-.94	.24	-1.12	.20	-.96	.30	-.99	.33	-1.28	.26	-.97	.33	-1.01	.36	-1.35	.30
25	-.82	.24	.70	.15	-.83	.25	-.86	.27	-1.04	.22	-.83	.28	-.87	.29	-1.13	.25
30	-.71	.24	.55	.15	-.71	.22	-.73	.24	-.87	.17	-.73	.24	-.76	.26	-.94	.22
35	-.59	.18	.50	.10	-.64	.19	-.64	.21	-.73	.16	-.65	.22	-.68	.23	-.78	.19
40	-.59	.12	.45	.10	-.58	.16	-.59	.19	-.62	.13	-.59	.19	-.61	.21	-.65	.16
45	-.47	.12	.40	.10	-.52	.13	-.53	.16	-.55	.12	-.53	.17	-.54	.18	-.56	.14
50	-.47	.12	.40	.10	-.45	.13	-.47	.14	-.46	.09	-.46	.15	-.48	.16	-.48	.12
55	-.35	.06	.30	.05	-.41	.12	-.41	.13	-.42	.09	-.41	.14	-.43	.15	-.42	.10
60	-.35	0	.25	.05	-.35	.10	-.36	.13	-.36	.06	-.36	.13	-.37	.14	-.36	.10
65	-.29	0	.25	0	-.30	.09	-.30	.10	-.32	.06	-.31	.12	-.32	.13	-.32	.08
70	-.24	.06	.20	0	-.26	.09	-.27	.10	-.28	.04	-.27	.11	-.28	.12	-.28	.07
75	-.18	0	.15	0	-.20	.07	-.21	.09	-.23	.03	-.21	.11	-.22	.11	-.24	.05
80	-.18	0	.15	0	-.16	.07	-.16	.09	-.20	.03	-.17	.11	-.18	.11	-.20	.05
85	-.12	0	.10	0	-.12	.07	-.11	.07	-.17	0	-.12	.09	-.13	.09	-.17	.04
90	-.06	0	.05	0	-.07	.07	-.07	.07	-.13	0	-.07	.09	-.07	.09	-.13	.03
95	0	0	0	0	-.02	.07	-.01	.07	-.10	0	0	.11	-.01	.09	-.09	.01

TABLE IV.- NACA 0006 AIRFOIL

| Chordwise station, percent chord	Pressure coefficient, P												
	R = 2,710,000				R = 4,580,000						R = 6,780,000			
	α=6.0°; c_N=0.639		α=6.5°; c_N=0.687		α=6.0°; c_N=0.713		α=6.5°; c_N=0.783		α=7.0°; c_N=0.778		α=6.0°; c_N=0.758		α=6.5°; c_N=0.766	
	Upper	Lower	Upper	Lower	Upper	Lower	Upper	Lower	Upper	Lower	Upper	Lower	Upper	Lower
0	-4.28	- - -	-2.80	- - -	-4.85	- - -	-5.79	- - -	-1.95	- - -	-5.26	- - -	-2.44	- - -
.1	-5.80	- - -	-3.35	- - -	-6.54	- - -	-7.37	- - -	-2.14	- - -	-7.14	- - -	-3.42	- - -
.25	-5.05	.23	-3.20	.40	-5.87	.08	-6.57	-.15	-2.16	.53	-6.12	.05	-2.43	.43
.5	-4.69	- - -	-3.05	- - -	-4.60	- - -	-4.86	- - -	-2.12	- - -	-4.77	- - -	-2.34	- - -
.75	-3.26	1.00	-2.80	1.00	-3.92	.97	-4.32	.95	-2.10	1.00	-4.19	.96	-2.28	.99
1.0	-3.10	- - -	-2.70	- - -	-3.47	- - -	-3.80	- - -	-2.09	- - -	-3.68	- - -	-2.26	- - -
1.5	-2.59	.95	-2.55	.95	-2.85	.97	-3.12	1.00	-2.09	.95	-3.01	.98	-2.23	.96
2	-2.23	- - -	-2.48	- - -	-2.47	- - -	-2.68	- - -	-2.10	- - -	-2.62	- - -	-2.21	- - -
2.5	-1.97	- - -	-2.38	- - -	-2.16	- - -	-2.35	- - -	-2.10	- - -	-2.30	- - -	-2.20	- - -
3	-1.80	.80	-2.30	.80	-1.96	.82	-2.13	.85	-2.12	.79	-2.10	.82	-2.18	.80
4	-1.56	- - -	-2.10	- - -	-1.69	- - -	-1.84	- - -	-2.12	- - -	-1.82	- - -	-2.13	- - -
5	-1.41	- - -	-1.93	- - -	-1.54	- - -	-1.68	- - -	-2.10	- - -	-1.66	- - -	-2.07	- - -
5.75	- - -	.54	- - -	.55	- - -	.59	- - -	.27	- - -	.59	- - -	.59	- - -	.58
7.5	-1.18	.49	-1.45	.50	-1.27	.50	-1.37	.53	-1.95	.50	-1.37	.51	-1.83	.51
10	-1.05	.41	-1.15	.43	-1.13	.43	-1.22	.46	-1.72	.44	-1.21	.44	-1.57	.44
15	-.82	.28	-.85	.30	-.89	.33	-.97	.35	-1.25	.34	-.96	.33	-1.14	.34
20	-.69	.23	-.70	.25	-.77	.25	-.83	.27	-.94	.25	-.82	.25	-.88	.26
25	-.62	.18	-.60	.20	-.66	.21	-.70	.23	-.74	.22	-.70	.21	-.71	.22
30	-.54	.15	-.53	.18	-.58	.18	-.61	.20	-.62	.18	-.61	.18	-.61	.20
35	-.49	.13	-.45	.15	-.51	.16	-.54	.17	-.53	.16	-.55	.16	-.54	.17
40	-.44	.13	-.43	.15	-.46	.14	-.48	.15	-.48	.14	-.50	.13	-.48	.15
45	-.36	.10	-.38	.10	-.40	.11	-.42	.13	-.42	.12	-.43	.12	-.42	.13
50	-.33	.08	-.35	.10	-.36	.11	-.37	.11	-.38	.10	-.39	.10	-.37	.11
55	-.28	.08	-.30	.08	-.32	.10	-.34	.11	-.35	.10	-.34	.10	-.33	.10
60	-.26	.08	-.25	.08	-.28	.10	-.30	.10	-.30	.09	-.31	.08	-.29	.09
65	-.23	.08	-.23	.08	-.26	.08	-.27	.08	-.28	.07	-.28	.08	-.26	.09
70	-.18	.08	-.20	.08	-.22	.08	-.22	.08	-.22	.06	-.23	.07	-.22	.07
75	-.15	.05	-.15	.05	-.18	.08	-.18	.08	-.19	.05	-.19	.07	-.18	.07
80	-.13	.03	-.13	.05	-.13	.08	-.15	.08	-.16	.04	-.15	.07	-.15	.06
85	-.08	.03	-.10	.05	-.10	- - -	-.10	- - -	-.12	- - -	-.11	- - -	-.11	- - -
90	-.03	.03	-.08	.05	-.05	.06	-.06	.06	-.10	.02	-.07	.05	-.08	.04
95	0	.03	0	.05	0	.07	-.01	.06	-.05	.02	-.02	.05	-.05	.03
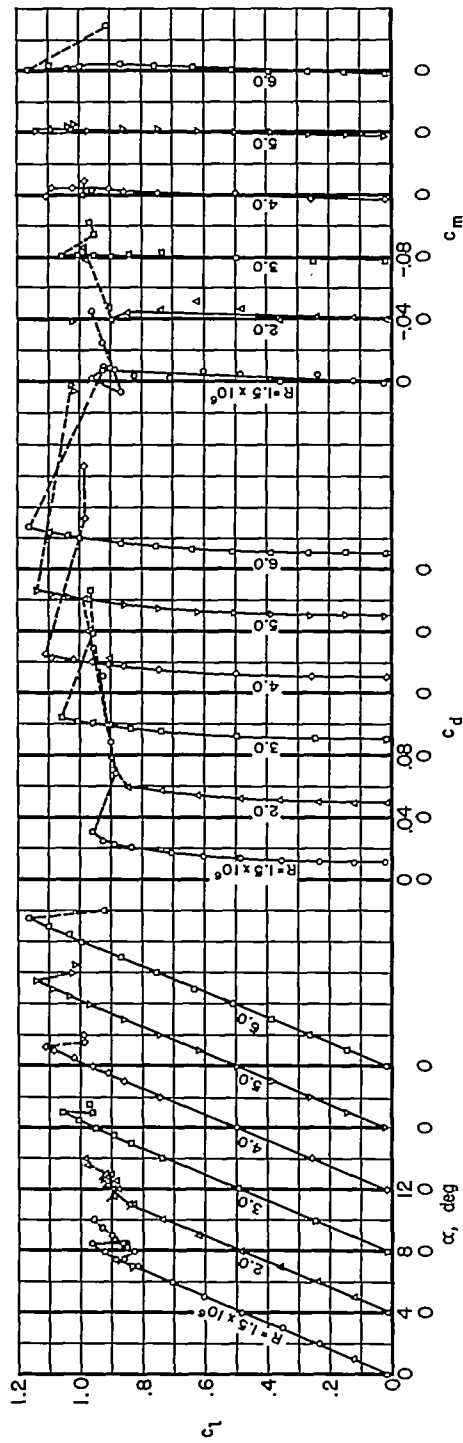
(a) NACA 0008 airfoil.
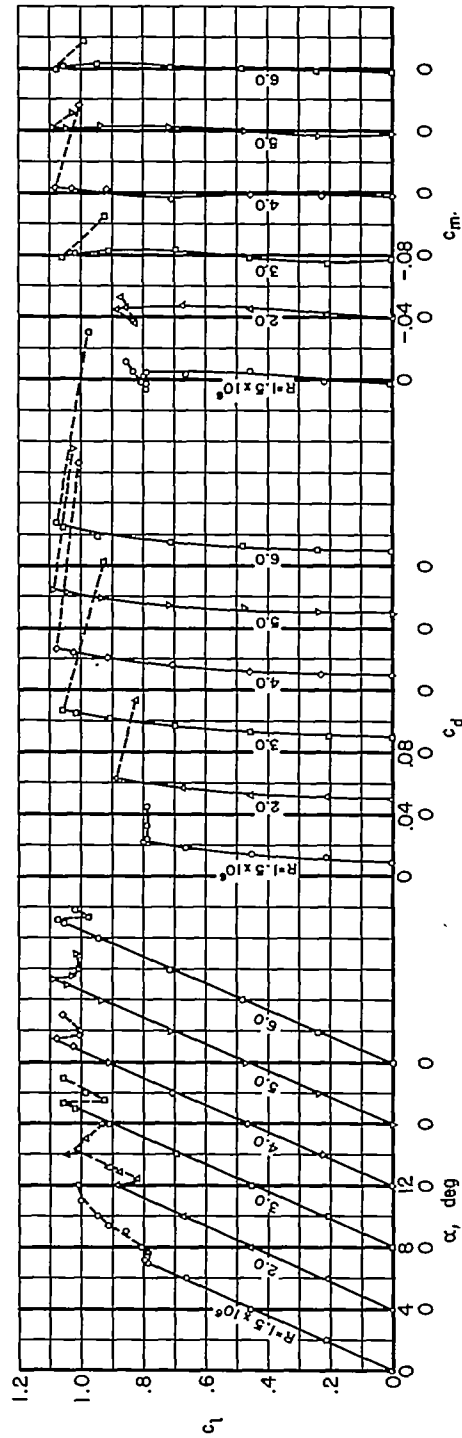
(b) NACA 0007.5 airfoil.

Figure 1.- Aerodynamic characteristics of four airfoils at several Reynolds numbers.
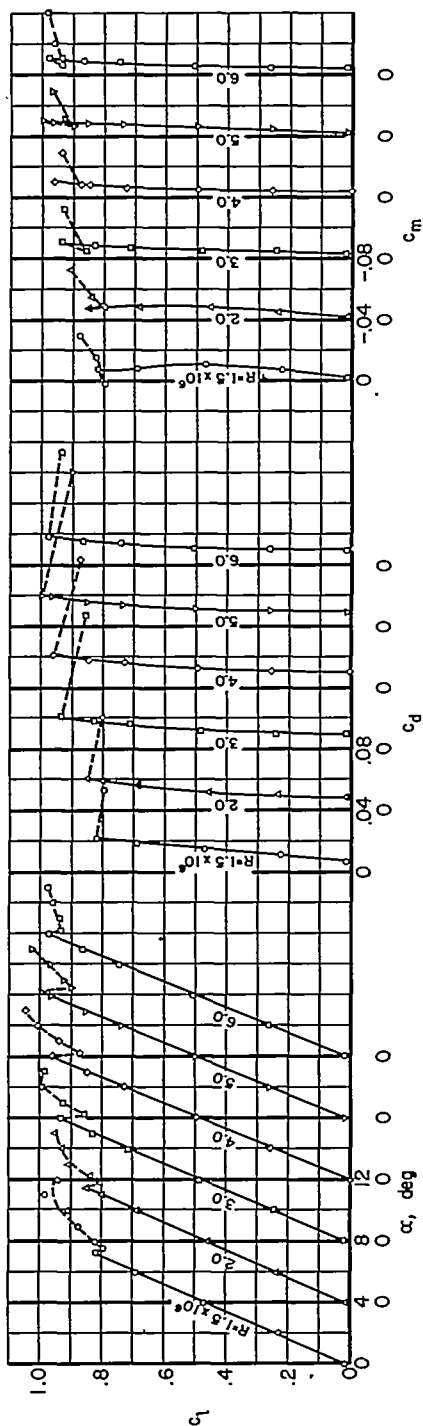
(c) NACA 0007 airfoil.
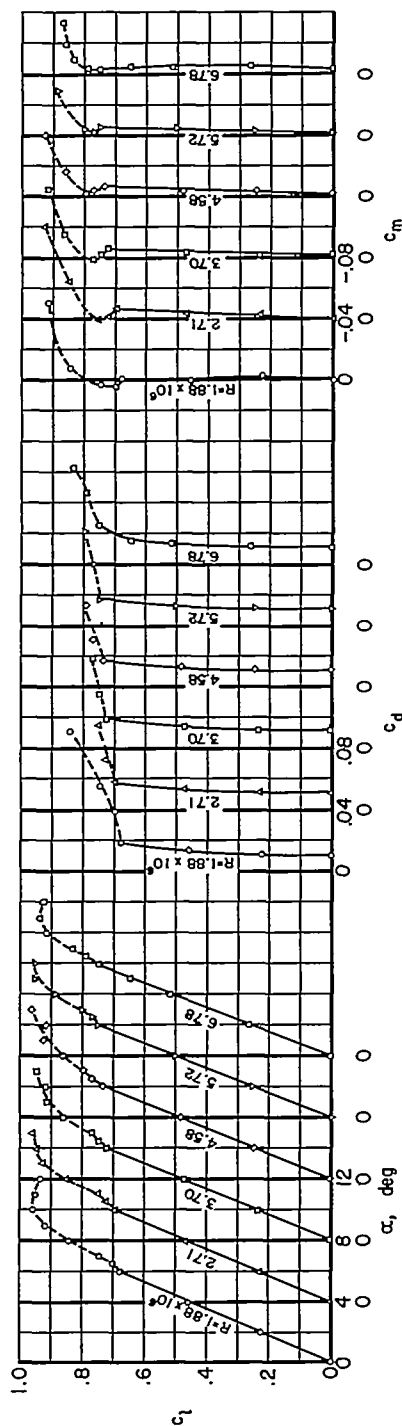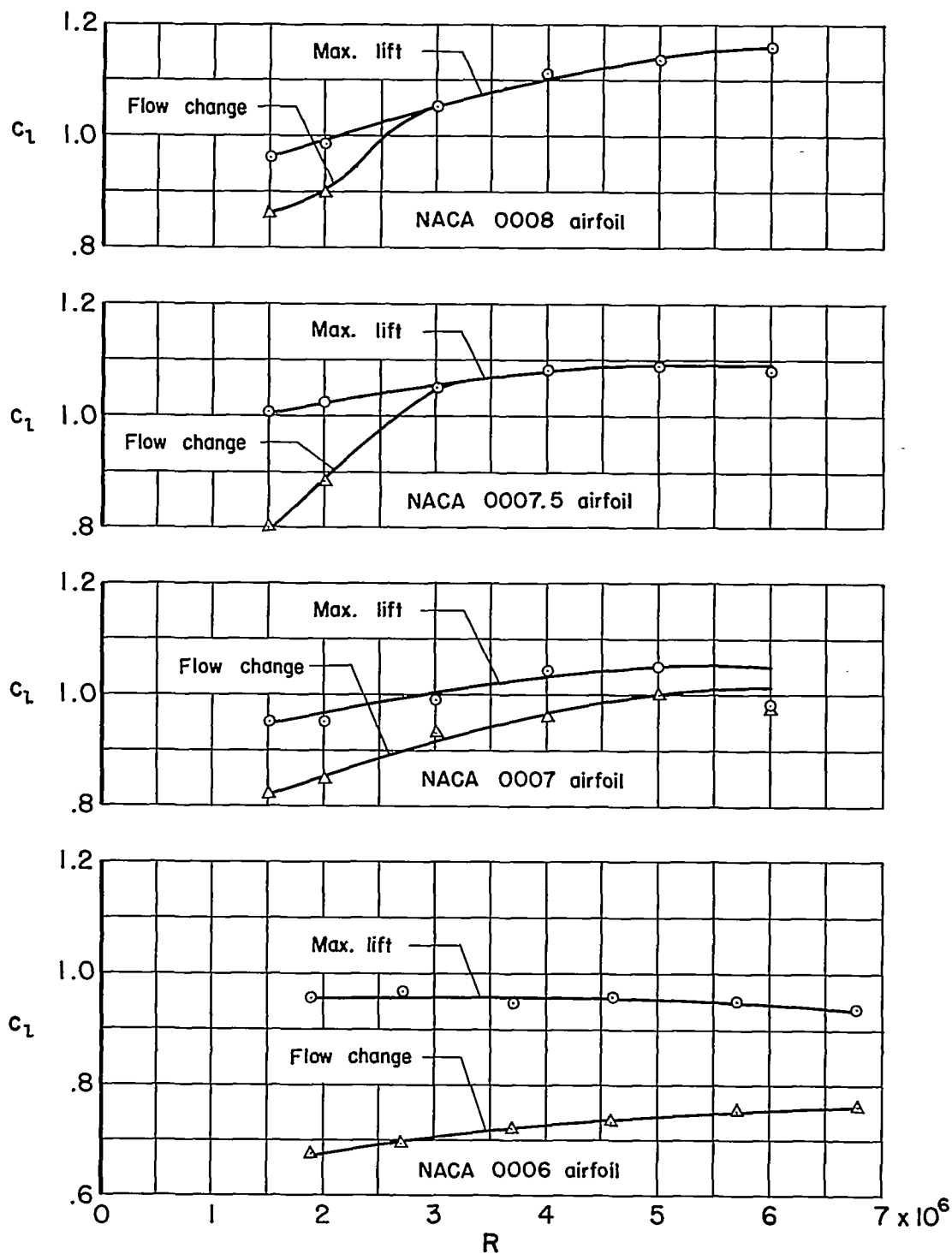
(d) NACA 0006 airfoil.

Figure 1.- Concluded.

Figure 2.- Variation of maximum lift and the lift corresponding to the flow change with Reynolds number.
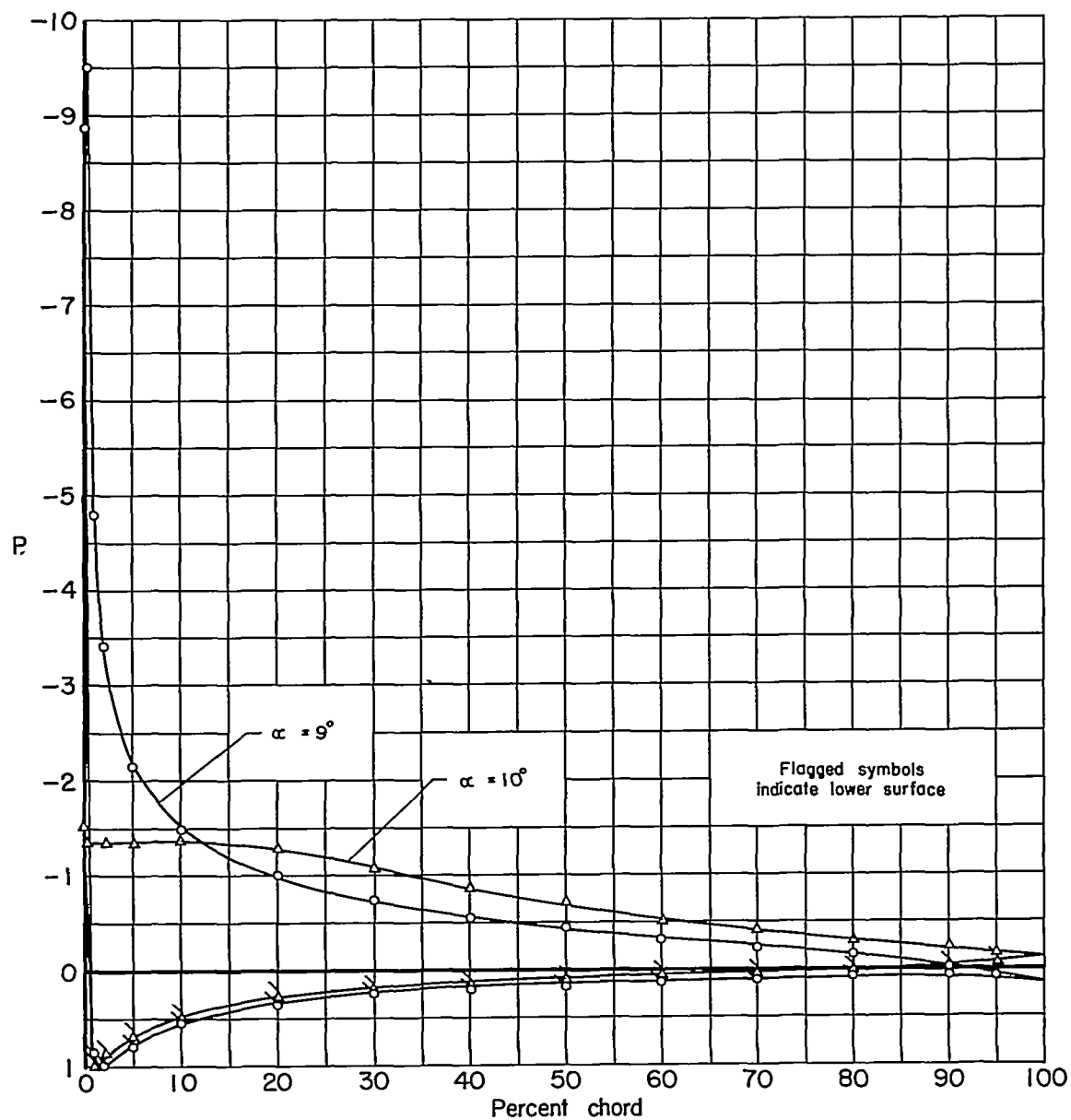
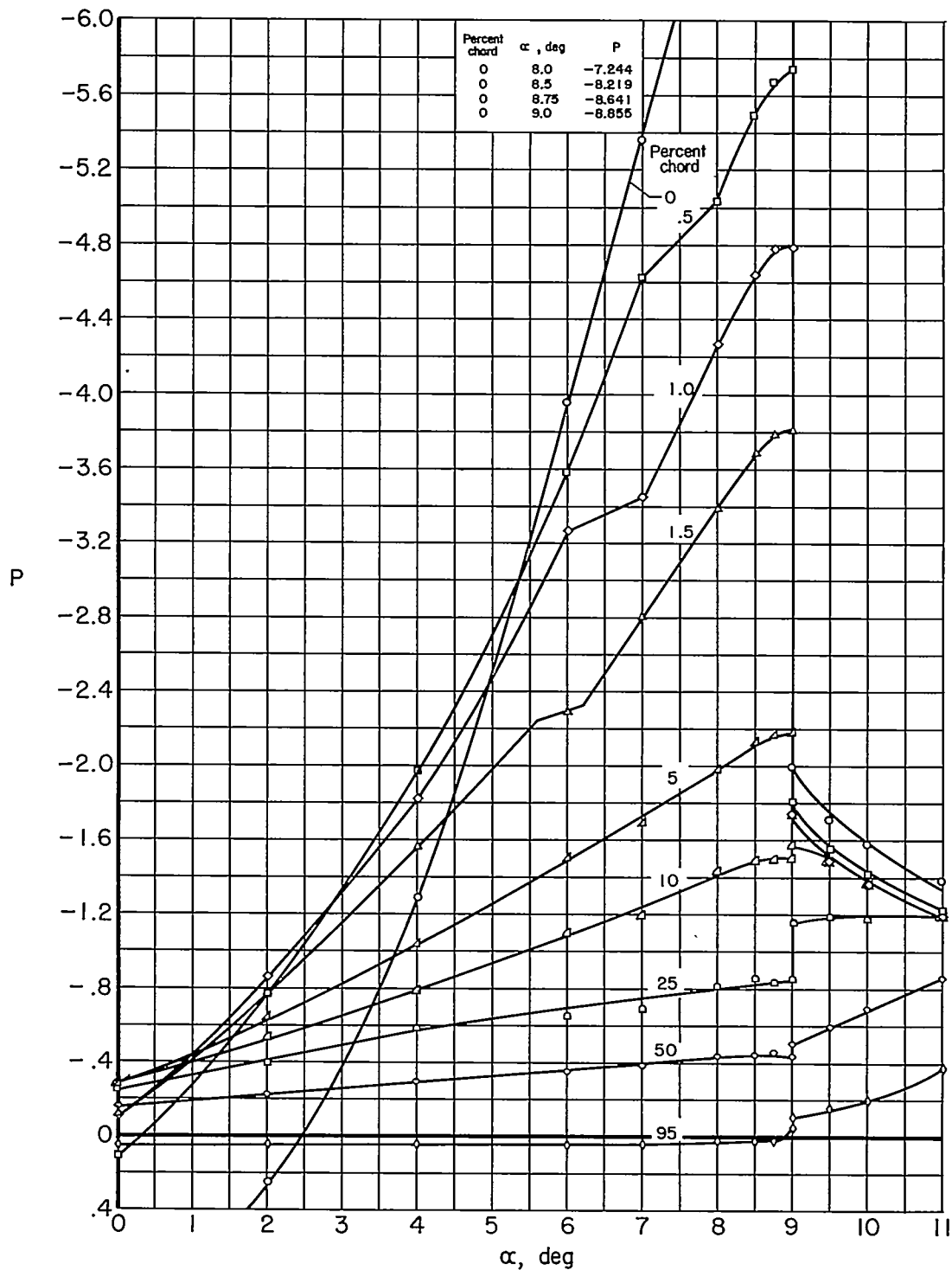Figure 3.- Chordwise distribution of pressure for the NACA 0007.5
airfoil; R = 3×10^6.

Figure 4.- Variation of pressure coefficient with angle of attack for various chordwise stations. NACA 0007.5 airfoil; R = 2×10⁶.
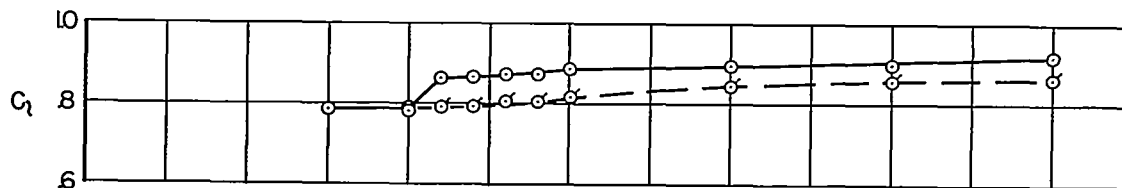
(a) c_l vs. Reynolds number.
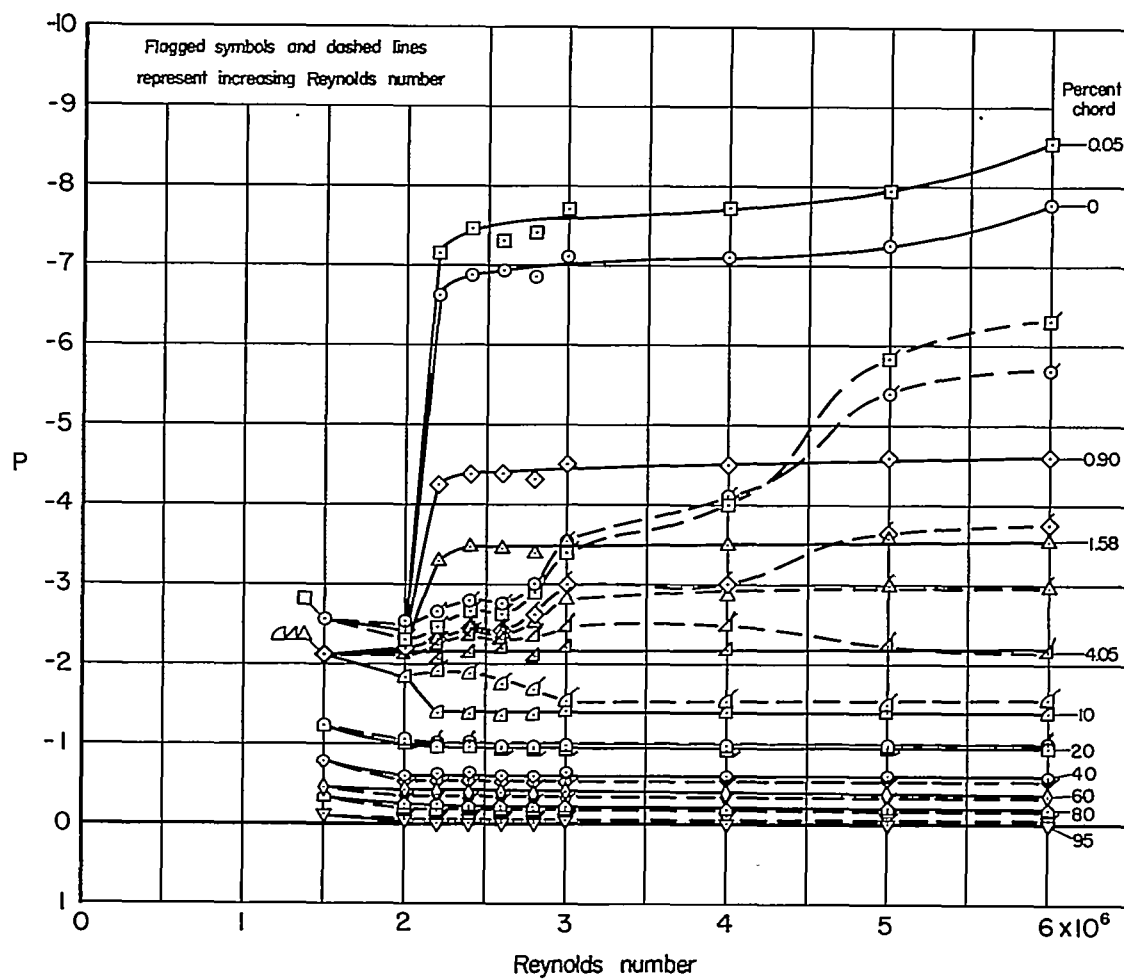
(b) P vs. Reynolds number.

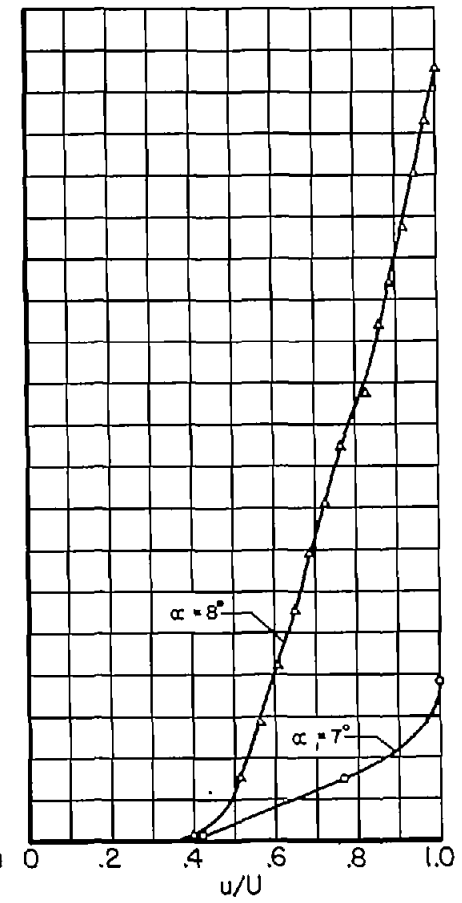Figure 5.- The effect of decreasing and increasing Reynolds number;
NACA 0007 airfoil; $\alpha = 7.5^\circ$.
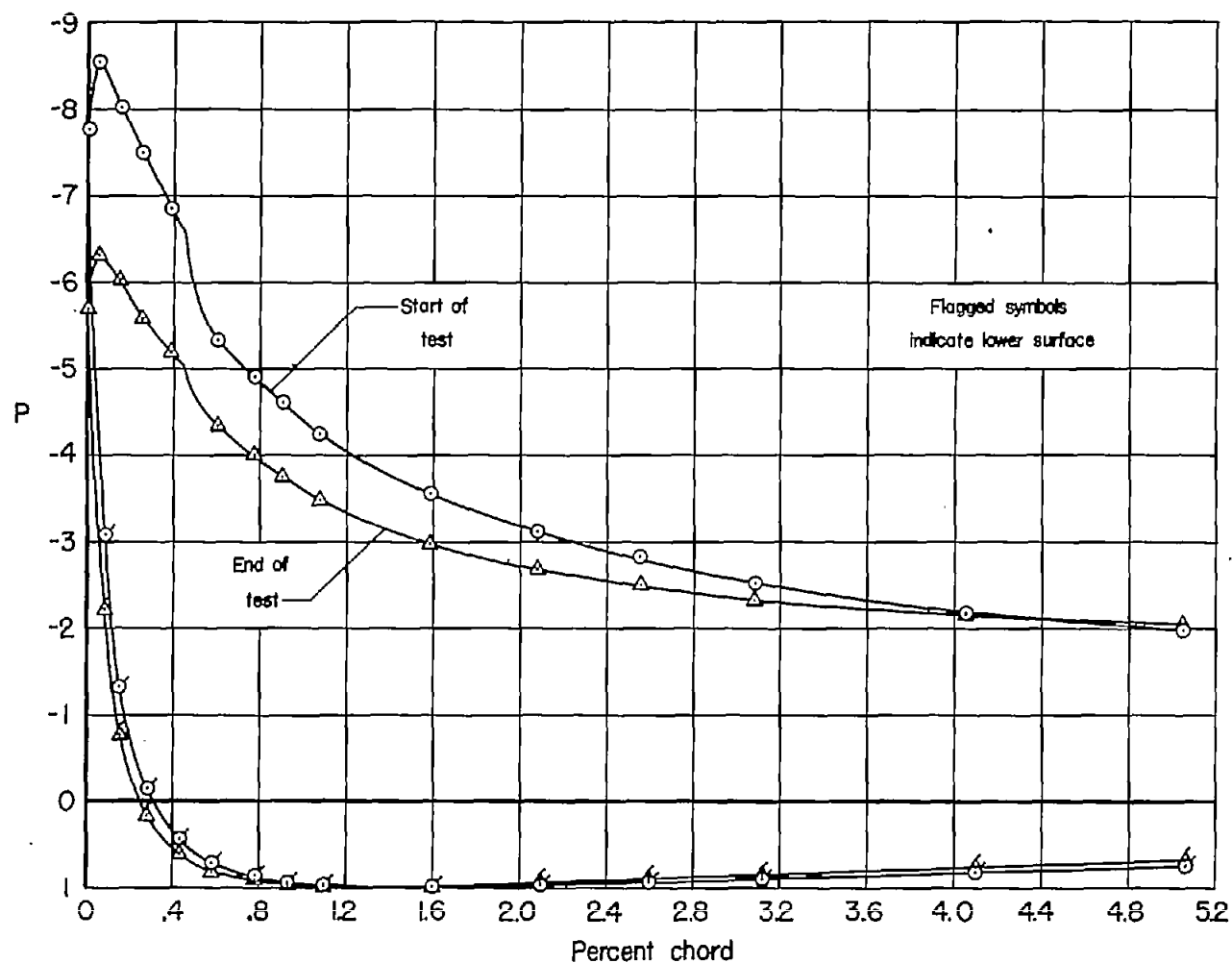
Figure 6.- Initial and final pressure distributions near the leading edge of the NACA 0007 airfoil; $R = 6 \times 10^6$; $\alpha = 7.5°$.
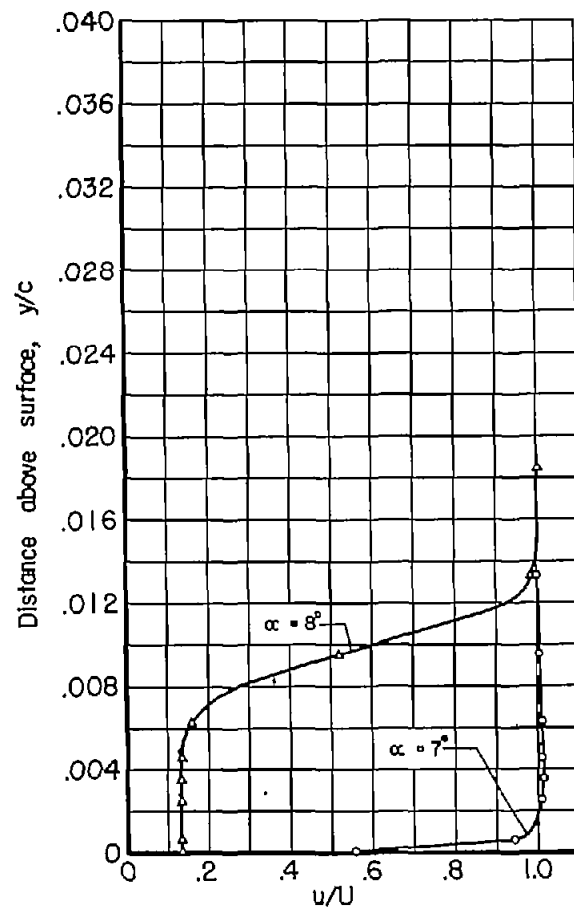
(a) 2.5-percent chord.
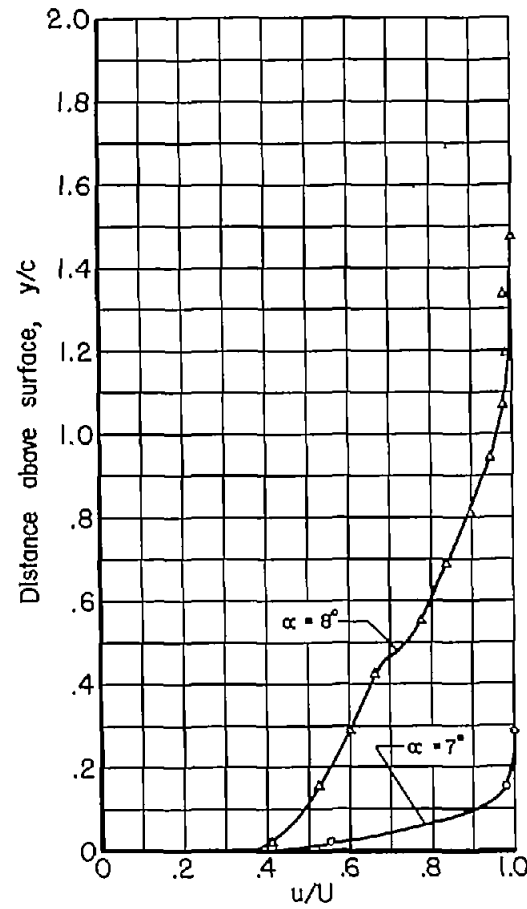
(b) 50-percent chord.

(c) 90-percent chord.

Figure 7.- Boundary-layer velocity profiles for the NACA 0007 airfoil; R = 2x10⁶.

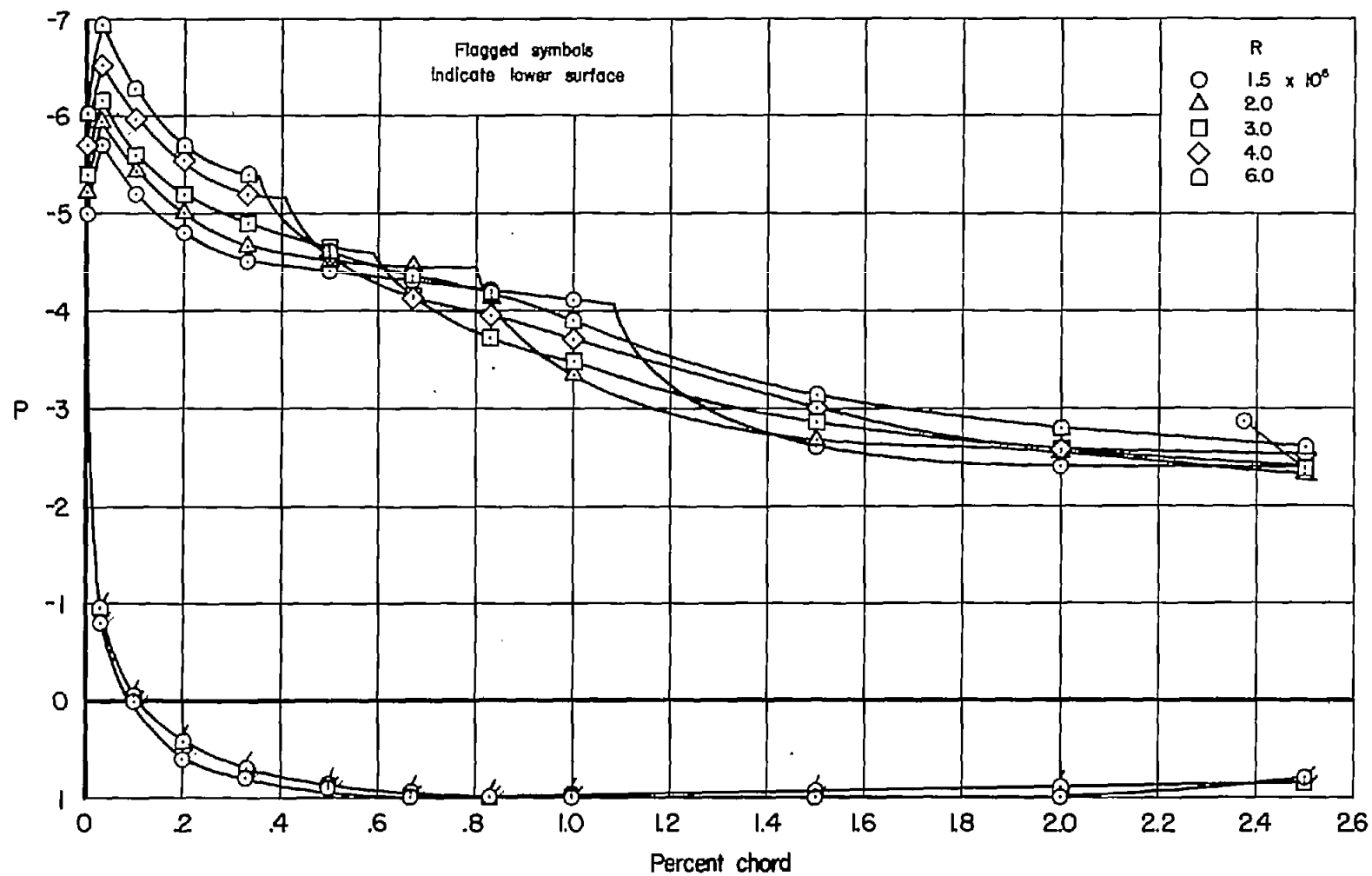Figure 8.- Details of the pressure distribution near the leading edge of the NACA 0007.5 airfoil; α = 7.0°.
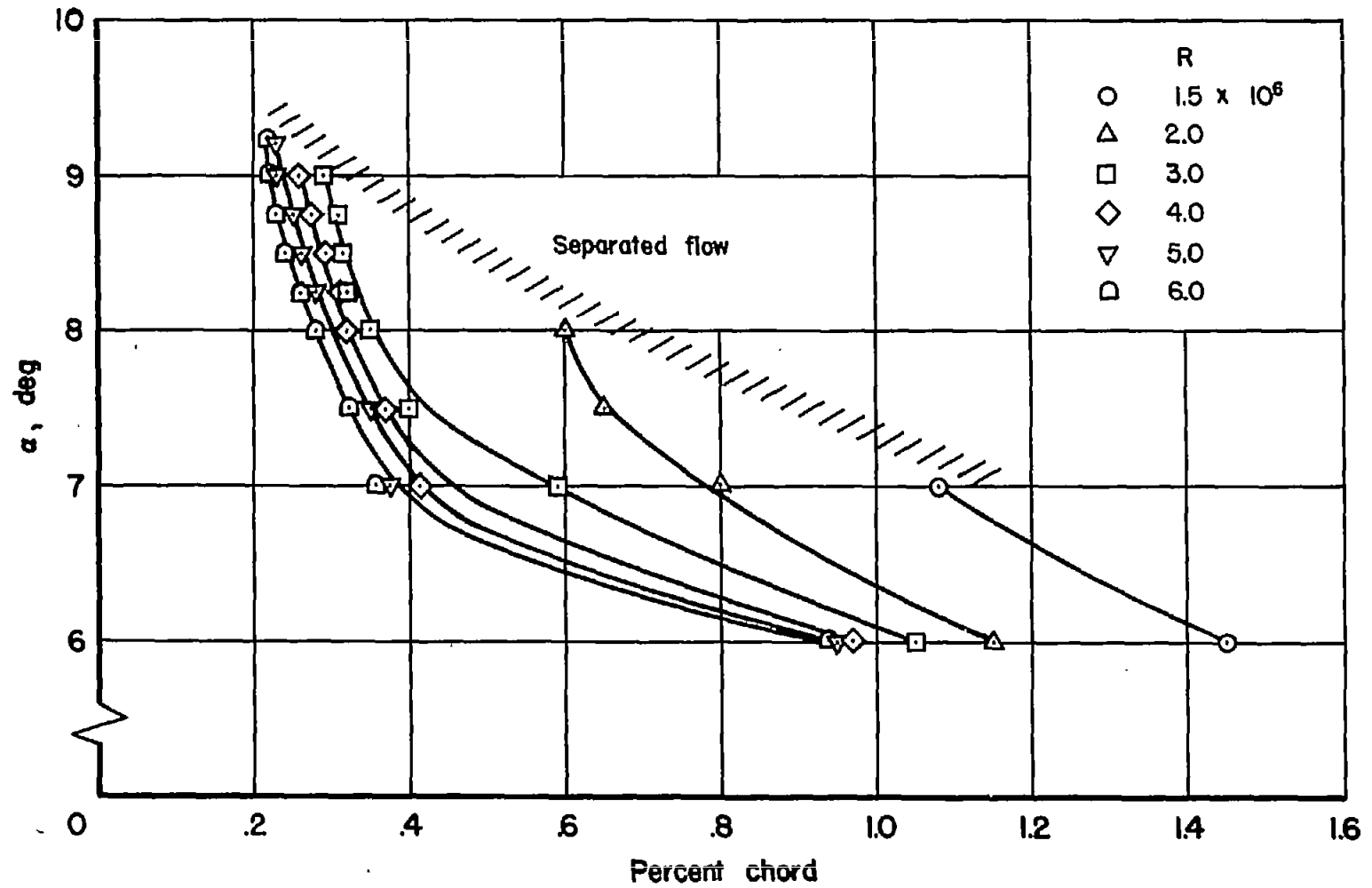
Figure 9.- Location of region of transition from laminar to turbulent flow on the NACA 0007.5 airfoil as indicated by pressure distribution.